



# Synthesis, characterization and photophysics of alkyne bridged bimetallic rhenium(I) and ruthenium(II) complexes

Murugesan Velayudham<sup>a</sup>, Subramanian Singaravadivel<sup>a</sup>, Seenivasan Rajagopal<sup>a,\*</sup>, Perumal Ramamurthy<sup>b</sup>

<sup>a</sup> Department of Physical Chemistry, School of Chemistry, Madurai Kamaraj University, Madurai 625 021, Tamil Nadu, India

<sup>b</sup> National Center for Ultrafast Processes, University of Madras, Taramani Campus, Chennai 600 113, Tamil Nadu, India

## ARTICLE INFO

### Article history:

Received 17 December 2008

Received in revised form 1 August 2009

Accepted 18 August 2009

Available online 21 August 2009

### Keywords:

Rhenium(I)

Ruthenium(II)

Bimetallic complex

Photophysics

Energy transfer

## ABSTRACT

Six new homobimetallic and heterobimetallic complexes of rhenium(I) and ruthenium(II) bridged by ethynylene spacer  $[(\text{CO})_3(\text{bpy})\text{Re}(\text{BL})\text{Re}(\text{bpy})(\text{CO})_3]^{2+}$ ,  $[\text{Cl}(\text{bpy})_2\text{Ru}(\text{BL})\text{Ru}(\text{bpy})_2\text{Cl}]^{2+}$  and  $[(\text{CO})_3(\text{bpy})\text{Re}(\text{BL})\text{Ru}(\text{bpy})_2\text{Cl}]^{2+}$  (bpy = 2,2'-bipyridine, BL = 1,2-bis(4-pyridyl)acetylene (bpa) and 1,4-bis(4-pyridyl)butadiyne (bpb) are synthesized and characterized. The electrochemical and photophysical properties of all the complexes show a weak interaction between two metal centers in heterobimetallic complexes. The excited state lifetime of the complexes is increased upon introduction of ethynylene spacer and the transient spectra show that this is due to delocalization of electron in the bridging ligand. Also, intramolecular energy transfer from  $^3\text{Re}(\text{I})$  to  $\text{Ru}(\text{II})$  in  $\text{Re}-\text{Ru}$  heterobimetallic complexes occurs with a rate constant  $4 \times 10^7 \text{ s}^{-1}$ .

© 2009 Published by Elsevier B.V.

## 1. Introduction

The simplest class of supramolecular architecture is a two component system called 'dyad' [1–3], in which the two components are connected by a bridge called spacer. The design and construction of multicomponent supramolecular systems has drawn much attention to mimic the function of natural photosynthesis and to study directional electron/energy transfer as well as electronic interaction across bridging ligands [4,5]. The tuning and optimization of such basic systems have gained tremendous interest due to the potential application of these supramolecular systems in the field of optical and electronic devices as wires [1,6,7] or switches [8] and in artificial light energy conversion [1,9,10]. It is interesting to go from molecular to supramolecular system, because the latter shows, in addition to the properties inherent of each molecular unit, the properties related to the structure and composition of whole unit [11–13].

The dyads are suitable for studies involving intramolecular electron/energy transfer process [14]. The energetics characteristics of these systems can be manipulated easily by choosing suitable mononuclear building blocks and appropriate bridging ligands and thereby the direction and the required rate of energy and electron transfer can be achieved [14,15]. An important requirement is that the bridge connecting the two components must be rigid, otherwise the results obtained are of limited interest because they

cannot be compared with the predictions of energy and electron transfer theories [12,14–16]. For photoinduced intramolecular energy transfer to occur, the dyad needs to contain two components. Among the two, one should have significantly higher excited state energy than the other, allowing the necessary gradient, and the lifetime of the donor must be long enough such that the energy transfer rate is faster than the intrinsic deactivation rate by luminescence. Photoinduced energy transfer is mostly probed by luminescence method. If both the donor and acceptor components are luminescent, then the rate of energy transfer can be determined from either the reduced emission lifetime of the energy donor unit or the rise time in the sensitized luminescence of the acceptor unit or both.

The  $d^6$  transition metal polypyridyl complexes of  $\text{Ru}(\text{II})$ ,  $\text{Os}(\text{II})$  and  $\text{Re}(\text{I})$ , because of favorable properties inherent on them, usually act as components in the dyad [1,3,7,14]. These metal complexes are highly luminescent and emit from the  $^3\text{MLCT}$  state, which has moderate excited state lifetime. They show high photostability and various redox states and possess the ability to undergo energy and electron transfer process. A large variety of spacers [7] are used to design multicomponent systems. They include flexible spacers like alkanes [9], rigid spacers like alkenes [17], alkynes [18], phenylenes [19], naphthalene [20], anthracene [20], thiophene [21], and alicyclics [22]. Metal complexes of  $\text{Ru}(\text{II})$  and  $\text{Os}(\text{II})$  based on rigid spacers of rod like acetylene are synthesized and studied extensively [23–25]. These rigid spacers provide desired features such as rigidity, electronic conductivity and coordination versatility [23,26]. Spacers made of fused aromatic rings are also

\* Corresponding author. Tel.: +91 452 2458246; fax: +91 452 2459139.  
E-mail address: [seenirajan@yahoo.com](mailto:seenirajan@yahoo.com) (S. Rajagopal).

used to connect the components made of metal complexes [27–29]. Cyclometalating rigid bridges are also used to study the photoinduced intramolecular electron/energy transfer processes [30].

Usually, heterobimetallic dyads are based on Ru(II) and Os(II) ions and a plethora of reports are available based on these ions [1,4,7,14]. However, Ru(II) and Re(I) heterobimetallic dyads are relatively less, though few reports are available [31–35]. In the present study, we describe the synthesis, photophysics and electrochemistry of rigidly bridged bimetallic complexes of ruthenium(II) and rhenium(I). An enormous amount of reports on multimetallic  $\text{Ru}^{\text{II}}(\text{bpy})_3$  type complexes based on the 2,2'-bipyridine ligands as the bridge are available in the literature [1,7]. In this work the bridge is directly attached to the metal center in monodentate fashion and another site is occupied by  $\text{Cl}^-$  ion.

## 2. Results and discussion

### 2.1. Synthesis

The structures of the bimetallic complexes used in the present study are shown in Chart 1. The bridging ligands were synthesized by sonogashira coupling reaction [36,37]. The complexes **I**, **IV** and

**VII** are available from our previous work [38,39]. The rhenium(I) complexes were synthesized from  $[\text{Re}(\text{CO})_3(\text{bpy})(\text{CH}_3\text{CN})](\text{CF}_3\text{SO}_3)$  [40] by converting  $\text{Re}(\text{CO})_3(\text{bpy})\text{Br}$  using  $\text{AgCF}_3\text{SO}_3$  in  $\text{CH}_3\text{CN}$ . The ruthenium(II) complexes were synthesized from  $[\text{Ru}(\text{bpy})_2(\text{NO})\text{Cl}](\text{PF}_6)$  [41]. The complexes were characterized by  $^1\text{H}$  NMR, ESI-MS and IR spectral techniques, in addition to elemental analysis.

### 2.2. ESI-MS

These complexes were characterized by ESI-MS technique. They show  $m/z$  values corresponding to the loss of one  $\text{PF}_6^-$  ion to give a monocharged species. Some of the monocharged species are given here,  $[\text{Cl}(\text{bpy})_2\text{Ru}(\text{bpa})\text{Ru}(\text{bpy})_2\text{Cl}](\text{PF}_6)$   $m/z$  1220,  $[(\text{CO})_3(\text{bpy})\text{Re}(\text{bpa})\text{Re}(\text{bpy})(\text{CO})_3](\text{PF}_6)$   $m/z$  1178,  $[\text{Cl}(\text{bpy})_2\text{Ru}(\text{bpb})\text{Ru}(\text{bpy})_2\text{Cl}](\text{PF}_6)$   $m/z$  1245,  $[(\text{CO})_3(\text{bpy})\text{Re}(\text{bpb})\text{Re}(\text{bpy})(\text{CO})_3](\text{PF}_6)$   $m/z$  1202 and  $[(\text{CO})_3(\text{bpy})\text{Re}(\text{bpa})\text{Ru}(\text{bpy})_2\text{Cl}](\text{PF}_6)$   $m/z$  1200 and  $[(\text{CO})_3(\text{bpy})\text{Re}(\text{bpb})\text{Ru}(\text{bpy})_2\text{Cl}](\text{PF}_6)$   $m/z$  1223. The ESI-MS spectra of **II**, **V**, **VI** and **VIII** are given in Figs. S1–S4 of Supplementary material. In the ESI-MS spectrum of **II** the peaks with  $m/z$  values 449, 490 and 629 are due to  $\text{Ru}(\text{bpy})_2\text{Cl}$ ,  $\text{Ru}(\text{bpy})_2\text{Cl}(\text{CH}_3\text{CN})$  and  $\text{Ru}(\text{bpy})_2\text{Cl}(4,4'\text{-bpy})$  species respectively. In **V** and **VI** the peaks with  $m/z$  values 427 and 468 correspond to  $\text{Re}(\text{bpy})(\text{CO})_3$  and  $\text{Re}(\text{bpy})(\text{CO})_3(\text{CH}_3\text{CN})$ , respectively. The peaks with  $m/z$  values 607 and 631 are due to  $\text{Re}(\text{bpy})(\text{CO})_3(\text{bpa})$  and  $\text{Re}(\text{bpy})(\text{CO})_3(\text{bpb})$ , respectively.

### 2.3. IR spectra

The infra-red spectra of rhenium(I) complexes are characterized by intense carbonyl stretching frequencies  $\nu(\text{CO})$  and the data are collected in Table 1. When we compare the IR spectra of homobimetallic rhenium(I) complexes **V** and **VI** with that of heterobimetallic complexes **VIII** and **IX**, only very little shift in the carbonyl stretching frequency is observed. This indicates that the interaction between the metal centers is weak.

### 2.4. Electrochemistry

The electrochemical behavior of the bimetallic complexes was studied in acetonitrile solution, and the relevant redox potentials are listed in Table 1. The ruthenium complex **II** shows oxidation wave with the  $E_{1/2}$  value 1.02 V. The DPV of **II** is given in Fig. S6 of Supplementary material. A single oxidation potential shows, two ruthenium(II) centers are in identical environment. When we compare the oxidation potential of ruthenium(II) homobimetallic complexes **II** and **III**, with that of **I** it is shifted to more positive value in the former complexes. This is because of the presence of electron withdrawing ethynylene group in **II** and **III**, which makes them difficult to oxidize. For **II** and **III**, in the cathodic

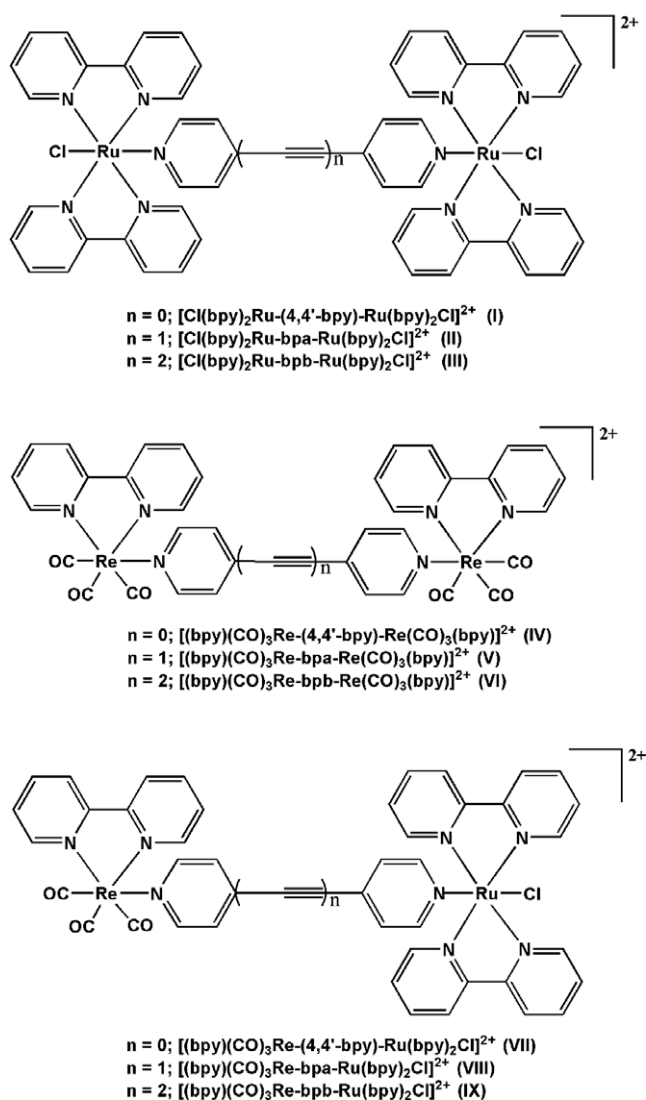


Chart 1. Structure of complexes.

Table 1  
IR spectral and electrochemical data<sup>a,b</sup> of bimetallic complexes.

Complex	$E_{1/2}$ (V)	$E_{1/2}$ (V)	$E_{1/2}$ (V)	$\nu(\text{CO})$ (cm <sup>-1</sup> )		
	Ru <sup>3+/2+</sup>	Re <sup>2+/+</sup>	Re <sup>+/0</sup>	bpy <sup>0/-</sup>	BL <sup>0/-</sup>	
<b>I</b>	+0.89			-1.30	-0.94	
<b>II</b>	+1.02			-1.26	-0.59	
<b>III</b>	+1.03			-1.28	-0.60	
<b>IV</b>		+1.68	-1.22	-1.06	-0.92	
<b>V</b>		+1.57	-1.45	-1.22	-0.63	2033, 1918
<b>VI</b>		+1.63	-1.29	-0.63	-0.63	2032, 1914
<b>VII</b>	+0.83	+1.80	-1.30	-1.06	-0.85	2030, 1920
<b>VIII</b>	+0.92	+1.46	-1.5	-1.29	-0.63	2032, 1917
<b>IX</b>	+0.97	+1.52	-1.45	-1.19	-0.70	2033, 1914

<sup>a</sup> In  $\text{CH}_3\text{CN}$ .

<sup>b</sup> Ag/AgCl reference electrode.

region, reduction occurs at considerably lower potential (−0.59 V) which can be assigned to the reduction of bridging ligand and other two subsequent reductions at large negative potentials can be assigned to the reduction of ancillary bipyridine ligands [42]. In the anodic scan, the rhenium(I) complexes **V** (Fig. 1) and **VI** (Fig. S7 in Supplementary material), show oxidation peak at +1.57 and +1.63 V corresponding to  $\text{Re}^{\text{I/II}}$ . In the cathodic region, the bridging ligand gets reduced first, followed by ancillary bipyridine ligand.

In the case of Re–Ru heterobimetallic complexes **VIII**, **IX**, in the anodic scan, two oxidation peaks are observed (Fig. 1 and Fig. S7 in Supplementary material). Based on the oxidation potentials of ruthenium(II) and rhenium(I) homobimetallic complexes, the oxidation peak at lower potential (ca. 0.92 V) is assigned to  $\text{Ru}^{\text{II/III}}$  oxidation and the peak at higher potential (ca. 1.5 V) is assigned to  $\text{Re}^{\text{I/II}}$  oxidation. When we compare the oxidation potential values of rhenium(I) component in heterobimetallic complexes **VIII** and **IX**, with that of rhenium(I) homobimetallic complexes **V** and **VI**, the oxidation potential of rhenium(I) metal center is shifted [43]. The oxidation potential of rhenium(I) center in heterobimetallic complexes **VIII** and **IX** is 110 mV shifted towards less positive value compared to homobimetallic complexes **V** and **VI**. This observed shift is because of increase in the electron density at the Re(I) unit by the electron withdrawing ‘ $\text{Re}(\text{CO})_3$ ’ core from Ru(II) unit. In the negative region, based on the comparison with homobimetallic complexes, first reduction is assigned to bridging ligand and other peaks are assigned to 2,2'-bipyridine ligand (Fig. S8).

### 2.5. Absorption spectra

The absorption spectra of all the complexes were recorded in  $\text{CH}_3\text{CN}$  at RT and the spectral data are collected in Table 2. The absorption spectra of bpa containing complexes **II**, **V** and **VIII** are shown in Fig. S9 of Supplementary material and of bpb containing complexes **III**, **VI** and **IX** in Fig. 2. For the ruthenium(II) complexes, the peaks at 290 nm and around 320 nm are assigned to  $\pi \rightarrow \pi^*$  transition associated with 2,2'-bpy and bridging ligand respectively. The peak seen in the visible region (ca. 487 nm) corresponds to  $^1\text{MLCT}$  transition [41].

The absorption at longer wavelength region indicates that the transition involved is  $\text{Ru}(\text{d}\pi) \rightarrow \text{BL}(\pi^*)$ . When we compare the absorption spectra of complexes **II** and **III** with that of **I** little shift in the  $\lambda_{\text{max}}$  value is observed. For the rhenium(I) complexes **V** and **VI**, ligand centered  $\pi \rightarrow \pi^*$  transitions corresponding to 2,2'-bpy and bridging ligand occur in the UV region. A shoulder seen in

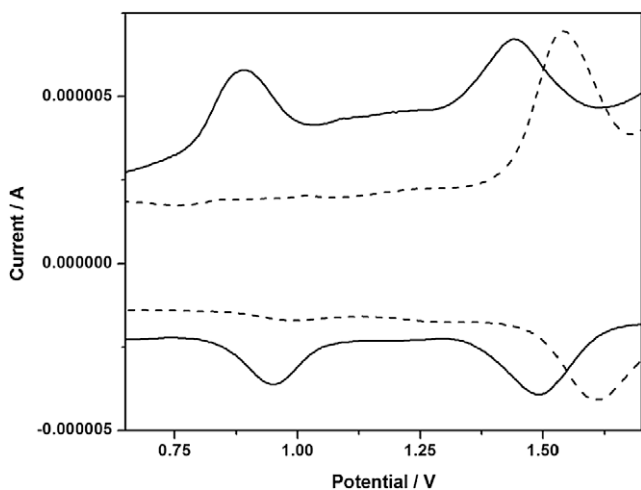


Fig. 1. Differential pulse voltammogram of **V** (...) and **VIII** (—) in  $\text{CH}_3\text{CN}$ .

Table 2  
Photophysical properties of bimetallic complexes in  $\text{CH}_3\text{CN}$  at 298 K.

Complex	$\lambda_{\text{max}}$	$\lambda_{\text{em, max}}$	$\tau$ (ns)	$\Phi_{\text{em}}$ ( $10^{-1}$ )	$k_r$ ( $10^4$ )	$k_{\text{nr}}$ ( $10^6$ )
<b>I</b>	291, 354, 489	726	28	0.023	7.8	35.0
<b>II</b>	292, 354, 487	700	30	0.009	3.0	33.3
<b>III</b>	291, 323, 489	672	33	0.013	3.9	30.0
<b>IV</b>	268, 306, 350	580	270	0.29	12	3.6
<b>V</b>	308, 319, 354	591	380	0.400	10.5	2.5
<b>VI</b>	308, 318, 353	591	893	0.600	6.7	1.1
<b>VII</b>	297, 341, 412	589	330	0.35	11	2.9
<b>VIII</b>	287, 320, 423	611	290	0.024	8.3	3.3
<b>IX</b>	289, 318, 425	613	545	0.032	5.9	1.8

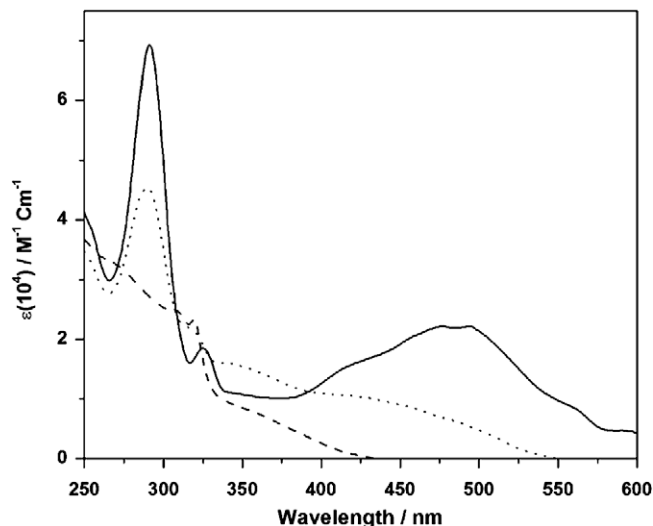


Fig. 2. Absorption spectra of complexes **III** (—), **VI** (---) and **IX** (····), recorded in  $\text{CH}_3\text{CN}$  at RT.

the region 350–355 nm is assigned to  $^1\text{MLCT}$  absorption. Except the absorption due to the ethynylene bridging ligand, the absorption spectra of **V** and **VI** are similar to that of **IV**. The absorption spectra of heterobimetallic complexes **VIII** and **IX** are shown in Fig. S9 of Supplementary material and Fig. 2, respectively. The peaks in the UV region, at 290 and 317–318 nm, are assigned to ligand centered transition associated with 2,2'-bpy and bridging ligand respectively. The peak in the visible region at ca. 422–425 nm is assigned to  $^1\text{MLCT}$  transition.

When we compare the absorption spectrum of **VIII** with that of **II**, a 64 nm blue shift is observed. Similar observation is noted in **IX** when compared with **III**. This blue shift is because of the attachment of electron withdrawing  $\text{Re}(\text{CO})_3$  unit into  $\text{Ru}^{\text{II}}$  unit. This trend, observation of blue shift, is also seen in  $\text{Re}^{\text{I}}\text{--Ru}^{\text{II}}$  heterobimetallic complex with 4,4'-bipyridine bridging ligand **VII** [39]. The blue shift is seen in related ruthenium(II) and osmium(II) complexes when more  $\pi$ -accepting ligands like triphenyl phosphine is attached [43].

### 2.6. Emission spectra

The emission spectra of all the complexes were measured in deoxygenated  $\text{CH}_3\text{CN}$  at RT and data are given in Table 2. For the ruthenium(II) complexes **II** and **III**, the emission maxima occur at 700 and 672 nm respectively upon excitation at wavelength corresponding to their MLCT absorption. The emission spectra of **II** and **III** are shown in Fig. S10 of Supplementary material and Fig. 3, respectively. Irrespective of excitation wavelength, same emission maximum is observed.

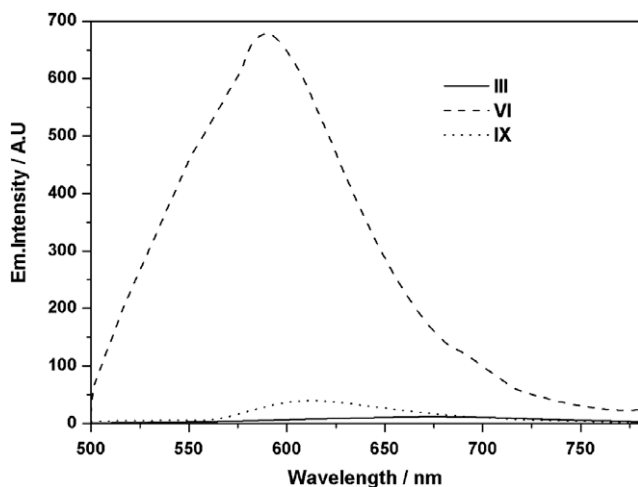


Fig. 3. Emission spectra of **III** (—), **VI** (---), and **IX** (...) recorded in degassed  $\text{CH}_3\text{CN}$  at RT.

The absorption spectra reveal that MLCT state is localized at the bridging ligand and hence the energy level responsible for the emission is assigned to  $^3\text{MLCT}$  state localized on the bridging ligand. Upon excitation at 350 nm, rhenium(I) complexes show emission from  $^3\text{MLCT}$  state with emission maximum at 590 nm (Fig. 3 and Fig. S10). When we compare the emission maxima of complexes **V** and **VI** with that of rhenium(I) homobimetallic complex having 4,4'-bipyridine bridging ligand **IV**, which has the emission maximum at 580 nm, a red shift to a tune of 10 nm is observed in the former complexes. This red shift can be attributed to the stabilization of  $^3\text{MLCT}$  state upon addition of ethynylene group. However, no appreciable shift in the emission maximum is observed on adding second ethynylene group.

When we look into the emission spectra of heterobimetallic complexes **VIII** and **IX**, (Fig. S10 and Fig. 3) the emission intensity is quenched compared to rhenium(I) homobimetallic complexes **V** and **VI**. The quenching of emission intensity can be explained by energy transfer from  $^3\text{Re(I)}$  to  $\text{Ru(II)}$  [31–34]. The electron transfer quenching can be ruled out on the basis of the result observed from the excitation spectra. The uncorrected excitation spectrum of **IX**, recorded with an emission wavelength of 610 nm, is shown in Fig. 4, which matches closely the absorption spectrum. This indi-

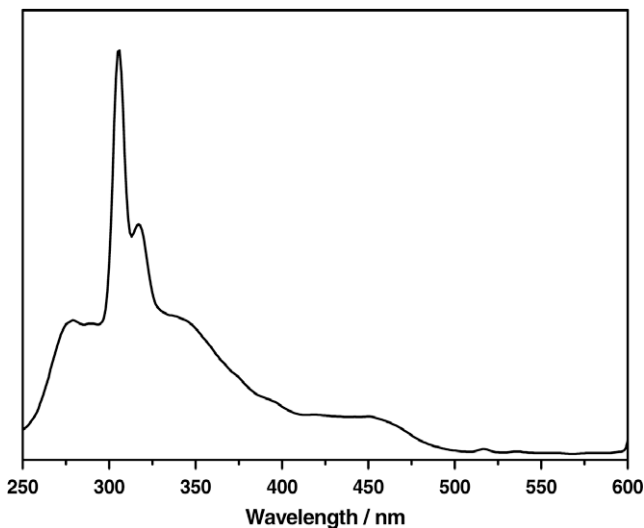


Fig. 4. Excitation spectrum of **IX** in  $\text{CH}_3\text{CN}$ .

cates that no photochemical reaction was observed following irradiation of the complex in the UV–Vis region.

Also the emission spectra of **VIII** and **IX** are blue shifted when compared with ruthenium(II) homobimetallic complexes **II** and **III**. A blue shift to a magnitude of 89 and 59 nm is observed in **VIII** and **IX** respectively. Similar trend is seen in the rhenium(I)–ruthenium(II) heterobimetallic complex with 4,4'-bipyridine bridging ligand [39].

## 2.7. Excited state lifetime and quantum yield

The excited state lifetimes of all the complexes were recorded in  $\text{CH}_3\text{CN}$  and collected in Table 2. The lifetime of **I** is 28 ns and is slightly increased when we introduce ethynylene bridging ligand in **II** and **III**. On the other hand the lifetime of rhenium(I) complexes **V** and **VI**, upon introduction of ethynylene group, is increased substantially compared to rhenium(I) homobimetallic complex **IV** (Table 2). Though the increase in the excited state lifetime of **V** is moderate, it is very much higher for **VI**. The increase in lifetime with a decrease in the energy gap can be explained in terms of electron delocalization occurring in the bridging ligand [24,44,45]. The quantum yield and the radiative ( $k_r$ ) and non-radiative rate constant ( $k_{nr}$ ) data were calculated and summarized in Table 2. Similar to excited state lifetime, the quantum yield of the rhenium complexes **V** and **VI** is increased compared to that of **IV**. Also the quantum yield of rhenium(I)–ruthenium(II) heterobimetallic complexes is increased compared to ruthenium(II) homobimetallic complexes. The increase in the lifetime and quantum yield of heterobimetallic complexes compared to ruthenium(II) homobimetallic complexes can be ascribed to energy transfer from  $^3\text{Re(I)} \rightarrow \text{Ru(II)}$  [31–34]. Since the energy level of MLCT state of rhenium(I) is higher than ruthenium(II),  $\text{Re(I)}$  acts as donor and  $\text{Ru(II)}$  acts as acceptor. Similar conclusion has been reached from the lifetime and quantum yield data in the case of dyad and triad complexes involving Pt, Ru and Os [46]. The increase in lifetime and quantum yield observed in the present study can be explained as detailed below similar to the previous report. For  $\text{Re–Ru}$  system, upon excitation at 340 nm  $^1\text{Re–L–Ru}$ ,  $\text{Re–}^1\text{L–Ru}$  and  $\text{Re–L–}^1\text{Ru}$  states are formed. The relaxed  $^3\text{Re–L–Ru}$  and  $\text{Re–}^3\text{L–Ru}$  states undergo fast energy transfer to  $\text{Re–L–}^3\text{Ru}$ . Therefore  $\text{Re–L–}^3\text{Ru}$  state receives contributions from direct 340 nm excitation and sensitisation by  $^3\text{Re–L–Ru}$  and  $\text{Re–}^3\text{L–Ru}$  states. Fig. 5 explains the various processes and energy levels involved in the system. From the excited state lifetime values the experi-

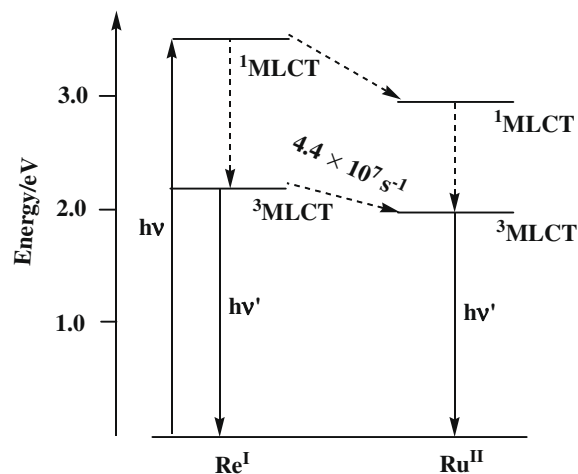


Fig. 5. Energy level diagram depicting energy transfer from  $^3\text{Re(I)}$  to  $\text{Ru(II)}$ .

mental energy transfer rate constant ( $k_{et}$ ) can be calculated by the following equation

$$k_{et} = (1/\tau) - (1/\tau^0) \quad (1)$$

where  $\tau^0$  is the excited state lifetime of rhenium(I) in **V** and **VI** and  $\tau$  is quenched lifetime of rhenium(I) in rhenium(I)–ruthenium(II) heterobimetallic complexes **VIII** and **IX**. The  $k_{et}$  values for **VIII** and **IX** are found to be  $4.4 \times 10^7$  and  $2.4 \times 10^7 \text{ s}^{-1}$ , respectively. Recently, Ward and co-workers [32] have studied intramolecular energy transfer process in a Re–Ru heterobimetallic complex by luminescence and time resolved infra-red (TRIR) techniques. They found intramolecular energy transfer from  $^3\text{Re(I)}$  to Ru(II) with a rate constant of  $ca. 1 \times 10^9 \text{ s}^{-1}$  and the increased rate of energy transfer observed in the complex may be due to the flexible nature of the bridge, which makes the donor and acceptor to come closer. Similar explanation can be offered to the systems studied by Furue et al. [34] who have obtained the energy transfer rate constant ranged from  $1.7 \times 10^8$  to  $1.2 \times 10^9 \text{ s}^{-1}$ .

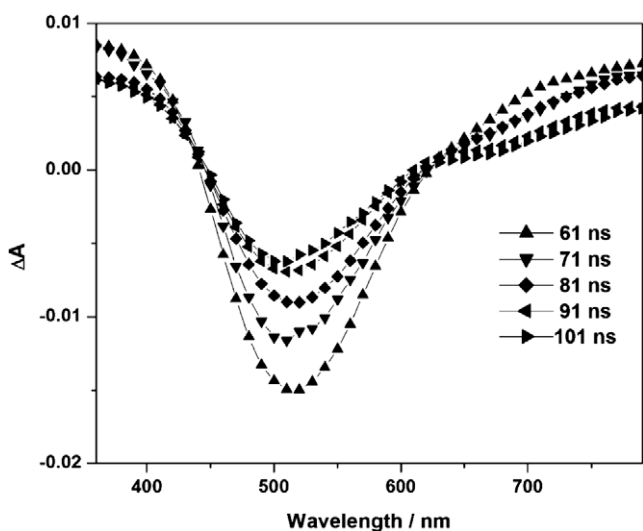
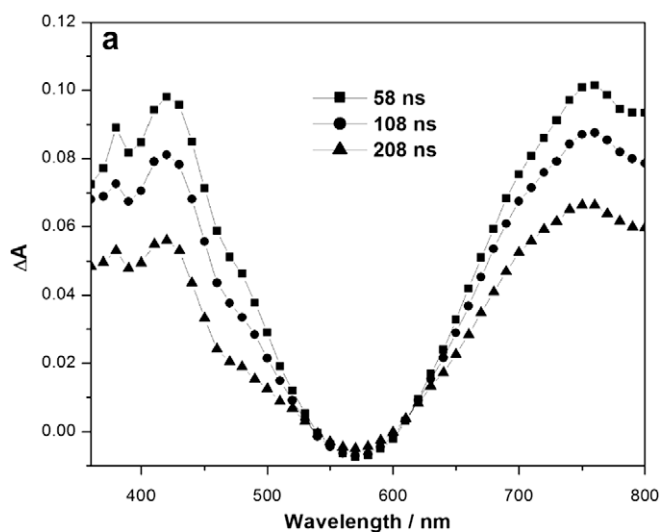


Fig. 6. Transient absorption spectra of **II** in degassed  $\text{CH}_3\text{CN}$  recorded at various time intervals after excitation at 355 nm.



## 2.8. Transient spectra

The transient absorption spectra of the ruthenium(II) complexes **II** and **III** are shown in Fig. 6 and Fig. S11 in Supplementary material. For the ruthenium(II) complexes **II** and **III**, upon excitation at 355 nm, absorption can be noticed at high energy region 370–420 nm and a broad absorption at low energy region 650–800 nm. The absorption in the longer wavelength region can be attributed to the  $\pi$  radical anion of the bridging ligand ( $\text{bpa}^-$  and  $\text{bpb}^-$ ) [42]. The  $\pi$  radical anion is produced, upon excitation, by charge transfer from Ru(II) to give  $\text{bpa}^-$  and  $\text{bpb}^-$ . The charge transfer from  $^3\text{Ru(II)}$  to bpa can be ascertained by the bleach seen in the region 490–540 nm. The bleach is due to the decay of ground state  $^1\text{MLCT}$  of Ru(II).

The transient spectrum of rhenium(I) complex **V** recorded at various time intervals is shown in Fig. 7a. For the rhenium(I) complex **V**, upon excitation at 355 nm, absorption occurs in the regions 370–420 and 700–750 nm. The absorption at the longer wavelength region can be attributed to the  $\pi$ -radical anion of the bridging ligand arising out of charge transfer from  $d\pi(\text{Re}) \rightarrow \pi^*(\text{bpa})$  to produce  $\text{bpa}^-$  [42]. The kinetic traces of decay of  $\pi$ -radical anion at 750 nm is shown in Fig. 7b and it decays with a lifetime of 400 ns.

The transient spectrum of rhenium(I) complex **VI**, recorded at various time intervals, is shown in Fig. S12 of Supplementary material. The transient spectrum is similar to that of the complex **V**. The complex **VI** shows absorption in the regions 400–540 nm and 680–800 nm, with latter being broad. The absorption is due to the generation of  $\pi$ -radical anion  $\text{bpb}^-$ .

The transient absorption spectra of rhenium(I)–ruthenium(II) heterobimetallic complexes **VIII** and **IX** are shown in Fig. 8 and Fig. S13 in Supplementary material. As noticed in the transient spectra of rhenium(I) and ruthenium(II) homobimetallic complexes, absorption is seen in the high energy region 380–480 nm and a broad absorption at longer wavelength region 680–780 nm. This absorption feature is characteristic of generation of anion radical of alkyne bridging ligands ( $\text{bpa}^-$  and  $\text{bpb}^-$ ). The formation of alkyne anion radical reveals that electron is delocalized on the bridging ligand. Though the bleach due to decay of Ru(II)  $^1\text{MLCT}$  state, because of energy transfer from  $^3\text{Re(I)}$  to Ru(II), is not clearly seen, it reveals that the time-scale of energy transfer is very short and could not be followed by nanosecond transient absorption measurement. However, emission spectral studies unambiguously showed occurrence of intramolecular energy transfer from  $^3\text{Re(I)}$  to

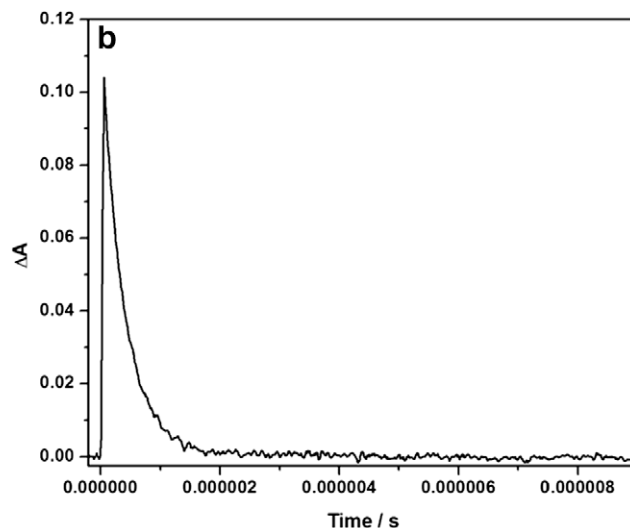


Fig. 7. (a) Transient absorption spectra of **V** in degassed  $\text{CH}_3\text{CN}$  recorded at various time intervals after excitation at 355 nm; (b) Kinetic profile of **V** recorded at 750 nm.

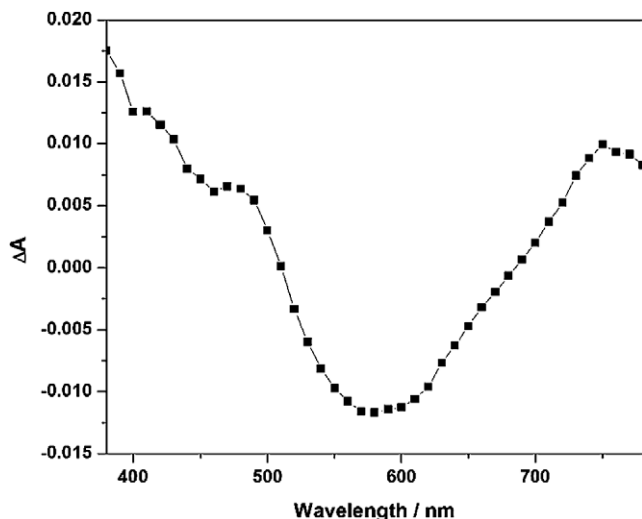


Fig. 8. Transient absorption spectra of VIII in degassed CH<sub>3</sub>CN recorded at 105 ns after excitation at 355 nm.

Ru(II) and in order to get more details about the excited state processes, picosecond transient absorption studies will be attempted. Energy transfer from <sup>\*</sup>Re(I) to Ru(II) can occur by Förster [47] or Dexter [48] mechanisms. The conjugated rigid bridge provides the through bond mechanism (Dexter) as the favorable one for energy transfer, however it is effective upto a distance of 10 nm. Since the bridging ligands distances are above 10 nm [41], the through space mechanism (Förster), which is operative upto 100 nm, cannot be ruled out.

### 3. Conclusions

A series of homobimetallic and heterobimetallic complexes of rhenium(I) and ruthenium(II) were synthesized and characterized. The electrochemical and photophysical behavior of all the complexes were studied and found that there is a weak interaction between rhenium(I) and ruthenium(II) metal centers in the heterobimetallic complexes. In the absorption and emission spectra, a blue shift is observed in heterobimetallic complexes compared to ruthenium(II) homobimetallic complexes, because of the attachment of 'Re(CO)<sub>3</sub>' unit in former. In the case of rhenium(I) homobimetallic complexes, lifetime is increased with increasing number of ethynylene groups and this is due to electron delocalization in the bridging ligand. Energy transfer from <sup>\*</sup>Re(I) to Ru(II) is observed in heterobimetallic complexes, which can be seen from the quenching of rhenium(I) based emission intensity in heterobimetallic complexes and also the excited state lifetime and quantum yield are increased for these complexes compared to ruthenium(II) homobimetallic complexes. In order to get further details about intramolecular energy transfer picosecond transient absorption studies will be attempted.

### 4. Experimental

#### 4.1. Materials

Re<sub>2</sub>(CO)<sub>10</sub> (Alfa), RuCl<sub>3</sub>·xH<sub>2</sub>O (Aldrich), 2,2'-bipyridine (Merck), AgCF<sub>3</sub>SO<sub>3</sub> (Alfa), 4-bromopyridine hydrochloride (Aldrich), 2-methyl-3-butyn-2-ol (Alfa), (PPh<sub>3</sub>)<sub>2</sub>PdCl<sub>2</sub> (Aldrich), copper(I) iodide (Merck) and NH<sub>4</sub>PF<sub>6</sub> (Alfa) were used as received. The bridging ligands 1,2-bis(4-pyridyl)acetylene (bpa) and 1,4-bis(4-pyridyl)buta-1,3-diyne (bpb) were synthesized by literature proce-

dures [36,37]. The complexes I and IV and VII were available from our previous work [38,39]. All solvents used for the synthesis were of reagent grade and for spectral measurements spectral grade was used.

#### 4.2. Syntheses

##### 4.2.1. Preparation of [Cl(bpy)<sub>2</sub>Ru(bpa)Ru(bpy)<sub>2</sub>Cl](PF<sub>6</sub>)<sub>2</sub> (II)

[Ru(bpy)<sub>2</sub>(NO)Cl](PF<sub>6</sub>)<sub>2</sub> (0.25 g, 0.32 mmol) was dissolved in acetone (25 mL) and to this was added dropwise a solution of KN<sub>3</sub> (0.05 g, 0.65 mmol) in MeOH. The reaction mixture was protected from light and stirred for 30 min. The solution was filtered through a glass frit to remove the insoluble KPF<sub>6</sub> salts. Then 1,2-bis(4-pyridyl)acetylene (bpa) (0.033 g, 0.18 mmol) was added to the acetone solution and it was refluxed for 24 h under argon blanket in dark. The volume of the acetone solution was reduced and added drop wise to anhydrous diethyl ether (125 mL) under vigorous stirring. The precipitate was filtered, washed and dried under vacuum. The product was further purified by column chromatography using alumina as the support and a mixture of toluene/CH<sub>3</sub>CN as the eluent. Yield = 62%. ESI-MS (*m/z*): 1220; <sup>1</sup>H-NMR (dms<sub>o</sub>-d<sub>6</sub>): 8.70 (8H, d), 8.23 (4H, d), 7.87 (8H, d), 7.60 (8H, t), 7.44 (4H, d), 7.19 (8H, t); Anal. Calc. for C<sub>52</sub>H<sub>40</sub>N<sub>10</sub>Cl<sub>2</sub>F<sub>12</sub>P<sub>2</sub>Ru<sub>2</sub>: C, 45.66; H, 2.95; N, 10.24. Found: C, 45.23; H, 2.67; N, 10.02%.

##### 4.2.2. Preparation of [Cl(bpy)<sub>2</sub>Ru(bpb)Ru(bpy)<sub>2</sub>Cl](PF<sub>6</sub>)<sub>2</sub> (III)

The compound was synthesized by adopting the procedure similar to the synthesis of II except that 1,4-bis(4-pyridyl)buta-1,3-diyne (bpb) was used as the bridging ligand. Yield = 64%. ESI-MS (*m/z*): 1245; <sup>1</sup>H-NMR (dms<sub>o</sub>-d<sub>6</sub>): 8.70 (8H, d), 8.21 (4H, d), 7.87 (8H, d), 7.62 (8H, t), 7.43 (4H, d), 7.19 (8H, t); Anal. Calc. for C<sub>54</sub>H<sub>40</sub>N<sub>10</sub>Cl<sub>2</sub>F<sub>12</sub>P<sub>2</sub>Ru<sub>2</sub>: C, 46.60; H, 2.90; N, 10.06. Found: C, 46.27; H, 2.58; N, 10.21%.

##### 4.2.3. Preparation of [(CO)<sub>3</sub>(bpy)Re(bpa)Re(bpy)(CO)<sub>3</sub>](PF<sub>6</sub>)<sub>2</sub> (V)

The reagents (bpy)(CO)<sub>3</sub>ReBr (0.25 g, 0.5 mmol) and AgCF<sub>3</sub>SO<sub>3</sub> (0.13 g, 0.5 mmol) were dissolved in CH<sub>3</sub>OH (25 mL) and refluxed for an hour under argon atmosphere. It was cooled to room temperature and filtered to remove AgBr. To the filtrate was added 1,2-bis(4-pyridyl)acetylene (bpa) (0.05 g, 0.27 mmol) and refluxed for 8 h under an argon blanket. The reaction mixture was evaporated to dryness and the solid redissolved in acetonitrile and loaded onto the alumina column. Elution was performed with a mixture of toluene/CH<sub>3</sub>CN. Initially 1:1 toluene/CH<sub>3</sub>CN was used to remove the unreacted 1,2-bis(4-pyridyl)acetylene and fac. [Re(bpy)(CO)<sub>3</sub>(CH<sub>3</sub>CN)](TFMS) and then the composition of the CH<sub>3</sub>CN is increased to collect the product. The product was then metathesized to PF<sub>6</sub><sup>-</sup> salt using NH<sub>4</sub>PF<sub>6</sub>. Yield = 64%. IR (KBr, cm<sup>-1</sup>): 2033, 1918; ESI-MS (*m/z*): 1178; <sup>1</sup>H-NMR (dms<sub>o</sub>-d<sub>6</sub>): 9.37 (4H, d), 9.10 (4H, d), 8.77 (4H, d), 8.41 (4H, m), 7.94 (4H, t), 7.76 (4H, d); Anal. Calc. for C<sub>38</sub>H<sub>24</sub>N<sub>6</sub>F<sub>12</sub>P<sub>2</sub>O<sub>6</sub>Re<sub>2</sub>: C, 34.50; H, 1.83; N, 6.35. Found: C, 34.63; H, 1.64; N, 6.14%.

##### 4.2.4. Preparation of [(CO)<sub>3</sub>(bpy)Re(bpb)Re(bpy)(CO)<sub>3</sub>](PF<sub>6</sub>)<sub>2</sub> (VI)

The compound was synthesized by adopting the procedure similar to V except that 1,4-bis(4-pyridyl)buta-1,3-diyne (bpb) was used as the bridging ligand. IR (KBr, cm<sup>-1</sup>): 2032, 1914; ESI-MS (*m/z*): 1202; <sup>1</sup>H-NMR (dms<sub>o</sub>-d<sub>6</sub>): 9.38 (4H, d), 9.19 (4H, d), 8.73 (4H, t), 8.42 (4H, m), 7.93 (6H, t), 7.77 (4H, d); Anal. Calc. for C<sub>40</sub>H<sub>24</sub>N<sub>6</sub>F<sub>12</sub>P<sub>2</sub>O<sub>6</sub>Re<sub>2</sub>: C, 35.67; H, 1.80; N, 6.24. Found: C, 35.33; H, 1.54; N, 6.37%.

##### 4.2.5. Preparation of [(CO)<sub>3</sub>(bpy)Re(bpa)Ru(bpy)<sub>2</sub>Cl](PF<sub>6</sub>)<sub>2</sub> (VIII)

To a degassed ethanol (60 mL), [(bpy)(CO)<sub>3</sub>Re(CH<sub>3</sub>CN)](CF<sub>3</sub>SO<sub>3</sub>) (0.13 g, 0.21 mmol) and [(bpy)<sub>2</sub>ClRu(bpa)](PF<sub>6</sub>) (0.16 g, 0.21 mmol) were dissolved and refluxed for 10 h under nitrogen atmosphere.

The reaction mixture was evaporated to dryness and the solid redissolved in minimum amount of EtOH and loaded onto the alumina column. Elution was performed with a mixture of toluene/EtOH. Initially 4:1 toluene/EtOH was used to remove the unreacted  $[\text{Re}(\text{bpy})(\text{CO})_3(\text{CH}_3\text{CN})](\text{CF}_3\text{SO}_3)$  and then the composition of the EtOH was increased to collect the product. The product was then metathesized to  $\text{PF}_6^-$  salt by dissolving in a minimum volume of acetone and then an aqueous solution of  $\text{NH}_4\text{PF}_6$  was added to get the precipitate. Yield = 65%. IR (KBr,  $\text{cm}^{-1}$ ): 2032, 1917; ESI-MS ( $m/z$ ): 1200;  $^1\text{H-NMR}$  ( $\text{dmsO-d}_6$ ): 8.77 (2H, d), 8.65 (6H, s), 8.56 (2H, d), 8.50 (2H, d), 8.17 (4H, t), 7.96 (6H, t), 7.80 (4H, m), 7.57 (2H, d), 7.52 (4H, d); Anal. Calc. for  $\text{C}_{45}\text{H}_{32}\text{N}_8\text{ClP}_2\text{F}_{12}\text{ReRu}$ : C, 41.66; H, 2.49; N, 8.64. Found: C, 41.32; H, 2.72; N, 8.46%.

#### 4.2.6. Preparation of $[(\text{CO})_3(\text{bpy})\text{Re}(\text{bpb})\text{Ru}(\text{bpy})_2\text{Cl}](\text{PF}_6)_2$ (**IX**)

The complex was synthesized by employing the procedure adopted for the complex **VIII**, except that  $[(\text{bpy})_2\text{ClRu}(\text{bpb})](\text{PF}_6)$  was used instead of  $[(\text{bpy})_2\text{ClRu}(\text{bpa})](\text{PF}_6)$ . Yield = 66%. IR (KBr,  $\text{cm}^{-1}$ ): 2033, 1914; ESI-MS ( $m/z$ ): 1223;  $^1\text{H-NMR}$  ( $\text{dmsO-d}_6$ ): 8.78 (2H, d), 8.66 (6H, d), 8.59 (2H, d), 8.50 (2H, d), 8.18 (4H, t), 7.95 (6H, t), 7.80–7.70 (4H, m), 7.59 (2H, d), 7.53 (4H, d); Anal. Calc. for  $\text{C}_{47}\text{H}_{32}\text{N}_8\text{ClP}_2\text{F}_{12}\text{ReRu}$ : C, 42.72; H, 2.44; N, 8.48. Found: C, 42.34; H, 2.19; N, 8.25%.

#### 4.3. Physical measurements

UV–Vis spectra were recorded on Analtikjena Specord S100 spectrophotometer and emission spectra were measured in JASCO FP6300 spectrofluorimeter. The concentration of the solution used was  $5 \times 10^{-5}$  M. All the samples used for emission were purged with dry nitrogen gas for about 20 min. The quantum yield of the complexes was calculated by using a degassed acetonitrile solution of  $[\text{Ru}(\text{bpy})_3]^{2+}$  as the standard ( $\Phi_{\text{em}} = 0.062$ ) [49]. IR spectra were measured using JASCO FT-IR spectrophotometer. The samples were recorded in the form of KBr pellets. The elemental analyses (C, H, N) were performed on Perkin–Elmer 2400.  $^1\text{H}$  NMR spectra were recorded using Bruker (Avance) 300 MHz NMR in  $\text{dmsO-d}_8$  and TMS as the internal standard. All the mass spectra were recorded using a Quattro LC triple-quadrupole mass spectrometer (Micro-mass, Manchester, UK) interfaced to an (Electro Spray ionization) ESI source; data acquisition was done under the control of MASSLYNX software (version 3.2). The ESI capillary voltage was maintained between 4.0–4.2 kV and the cone voltage kept at 25 V. Nitrogen was used as desolvation and nebulization gas. The source and desolvation temperatures were 100 °C.

#### 4.4. Electrochemistry

The redox potentials of the complexes were determined by cyclic voltammetric and differential pulse voltammetric techniques using EG & G Princeton Applied Research Potentiostat/Galvanostat Model 273 A. Measurements were performed by purging the solution in acetonitrile (spectroscopic grade) by dry nitrogen gas for 30 min. The supporting electrolyte is 0.1 M TBAH, Pt is the working electrode, and the  $\text{Ag}/\text{AgCl}$  is the reference electrode.

#### 4.5. Lifetime and transient measurements

The excited state lifetime measurements for all the complexes were made, after degassing the solutions with argon for 30 min, using time correlated single photon counting (TCSPC) technique and the details are given in previous reports [50,51]. Transient absorption measurements were made with laser flash photolysis technique as described elsewhere [50].

#### Acknowledgements

M.V. and S.R. thank Department of Science and Technology (DST), New Delhi, India for sanctioning a Project to carry out this research work and Dr. M. Vairamani for mass spectral measurements.

#### Appendix A. Supplementary material

Supplementary data associated with this article can be found, in the online version, at doi:10.1016/j.jorgchem.2009.08.025.

#### References

- [1] V. Balzani, G. Bergamini, P. Ceroni, *Coord. Chem. Rev.* 252 (2008) 2456.
- [2] S. Frayssé, C. Coudret, J.-P. Launay, *J. Am. Chem. Soc.* 125 (2003) 5880.
- [3] M. Beley, S. Chodorowski, J.-P. Collin, J.-P. Sauvage, L. Flamigni, F. Barigelletti, *Inorg. Chem.* 33 (1994) 2543.
- [4] V. Balzani, P. Bergamini, F. Marchioni, P. Ceroni, *Coord. Chem. Rev.* 250 (2006) 1245.
- [5] M.D. Ward, *Coord. Chem. Rev.* 251 (2007) 1663.
- [6] A.C. Benniston, *Chem. Soc. Rev.* 33 (2004) 573.
- [7] F. Barigelletti, L. Flamigni, *Chem. Soc. Rev.* 29 (2000) 1.
- [8] S. Sortino, S. Petralia, S. Conoci, S. Di Bella, *J. Am. Chem. Soc.* 125 (2003) 1122.
- [9] F. Puntoriero, S. Campagna, A.-M. Stadler, J.-M. Lehn, *Coord. Chem. Rev.* 252 (2008) 2480.
- [10] B. Hong, J.V. Ortega, *Angew. Chem., Int. Ed. Engl.* 37 (1998) 2131.
- [11] H. Hofmeier, U.S. Schubert, *Chem. Soc. Rev.* 33 (2004) 373.
- [12] A. Harriman, S.A. Rostron, A. Khatyr, R. Ziessel, *Faraday Discuss.* 131 (2006) 377.
- [13] E. Baranoff, J.-P. Collin, L. Flamigni, J.-P. Sauvage, *Chem. Soc. Rev.* 33 (2004) 147.
- [14] V. Balzani, A. Juris, M. Venturi, S. Campagna, S. Serroni, *Chem. Rev.* 96 (1996) 759.
- [15] M. Frank, M. Nieger, F. Vögtle, P. Belsler, A. von Zelewsky, L. De Cola, V. Balzani, F. Barigelletti, L. Flamigni, *Inorg. Chim. Acta* 242 (1996) 281.
- [16] F. Scandola, R. Argazzi, C.A. Bignozzi, M.T. Indelli, *J. Photochem. Photobiol. A: Chem.* 82 (1994) 191.
- [17] C.H. Tung, L.P. Zhang, Y. Li, H. Cao, Y. Tanimoto, *J. Am. Chem. Soc.* 119 (1997) 5348.
- [18] A. Harriman, A. Khatyr, R. Ziessel, A.C. Benniston, *Angew. Chem., Int. Ed.* 39 (2000) 4287.
- [19] B. Schlicke, P. Belsler, L. De Cola, E. Sabbioni, V. Balzani, *J. Am. Chem. Soc.* 121 (1999) 4207.
- [20] A. El-ghayoury, A. Harriman, A. Khatyr, R. Ziessel, *J. Phys. Chem. A* 104 (2000) 1512.
- [21] S. Encinas, L. Flamigni, F. Barigelletti, E.C. Constable, C.E. Housecroft, E.R. Shofield, E. Figgemeier, D. Fenske, M. Neuburger, J.G. Vos, M. Zehnder, *Chem. Eur. J.* 8 (2002) 137.
- [22] A. Juris, L. Prodi, A. Harriaman, R. Ziessel, M. Hissler, A. El-ghayoury, F. Wu, E.C. Riesgo, R. Thummel, *Inorg. Chem.* 39 (2000) 3590.
- [23] R. Ziessel, M. Hissler, A. El-ghayoury, A. Harriman, *Coord. Chem. Rev.* 178–180 (1998) 1251.
- [24] V. Grosshenny, A. Harriman, R. Ziessel, *Angew. Chem., Int. Ed. Engl.* 34 (1995) 1100.
- [25] A.C. Benniston, A. Harriman, P. Li, C.A. Sams, *J. Phys. Chem. A* 109 (2005) 2302.
- [26] T. Bartik, B. Bartik, M. Brady, R. Dembinski, J.A. Gladysz, *Angew. Chem., Int. Ed. Engl.* 35 (1996) 414.
- [27] J. Bolger, A. Gourdon, E. Ishow, J.-P. Launay, *Inorg. Chem.* 35 (1996) 2937.
- [28] E. Ishow, A. Gourdon, J.-P. Launay, P. Lecante, M. Verlest, C. Chiorboli, F. Scandola, C.A. Bignozzi, *Inorg. Chem.* 37 (1998) 3603.
- [29] M.-J. Kim, R. Konduri, H. Ye, F.M. MacDonnell, F. Puntoriero, S. Serroni, S. Campagna, T. Holder, G. Kinsel, K. Rajeshwar, *Inorg. Chem.* 41 (2002) 2471.
- [30] S. Ott, M. Borgström, L. Hammarström, O. Johansson, *Dalton Trans.* (2006) 1434.
- [31] A. Coleman, C. Brennan, J.G. Vos, M.T. Pryce, *Coord. Chem. Rev.* 252 (2008) 2585 (and references therein).
- [32] T.L. Easun, W.Z. Alsinidi, M. Towrie, K.L. Ronayne, X.-Z. Sun, M.D. Ward, M.W. George, *Inorg. Chem.* 47 (2008) 5071.
- [33] S. Van Wallendaal, D. Paul Rillema, *Coord. Chem. Rev.* 111 (1991) 297.
- [34] M. Furue, M. Naiki, Y. Kanematsu, T. Kushida, M. Kamachi, *Coord. Chem. Rev.* 111 (1991) 221.
- [35] B.J. Coe, E.C. Fitzgerald, M. Helliwell, B.S. Brunshwig, A.G. Fitch, J.A. Harris, S.J. Coles, P.N. Horton, M.B. Hursthouse, *Organometallics* 27 (2008) 2730.
- [36] L.D. Ciana, A. Haim, *J. Heterocyclic Chem.* 21 (1984) 607.
- [37] N.R. Champness, A.N. Khlobystov, A.G. Majuga, M. Schröder, N.V. Zyk, *Tetrahedron Lett.* 40 (1999) 5413.
- [38] M. Velayudham, M. Rajkumar, S. Rajagopal, P. Ramamurthy, *Polyhedron* 27 (2008) 3417.
- [39] M. Velayudham, S. Rajagopal, *Inorg. Chim. Acta* (2009), doi:10.1016/j.jica.2009.08.024.

- [40] R. Lin, Y. Fu, C.P. Brock, T.F. Guarr, *Inorg. Chem.* 31 (1992) 4346.
- [41] M.J. Powers, T.J. Meyer, *J. Am. Chem. Soc.* 102 (1980) 1289.
- [42] V. Grosshenny, A. Harriman, F.M. Romero, R. Ziessel, *J. Phys. Chem.* 100 (1996) 17472.
- [43] D. Xu, J.Z. Zhang, B. Hong, *J. Phys. Chem. A* 105 (2001) 7979.
- [44] A.C. Benniston, A. Harriman, F.M. Romero, R. Ziessel, *Dalton Trans.* (2004) 1233.
- [45] T. Rajendran, B. Manimaran, R.-T. Liao, R.-J. Lin, P. Thanasekaran, G.-H. Lee, S.-M. Peng, Y.-H. Liu, I.-Jy. Chang, S. Rajagopal, K.-L. Lu, *Inorg. Chem.* 42 (2003) 6388.
- [46] B. Ventura, A. Barbieri, F. Barigelletti, J.B. Seneclauze, P. Retailleau, R. Ziessel, *Inorg. Chem.* 47 (2008) 7048.
- [47] T. Förster, *Discuss. Faraday Soc.* 27 (1957) 7.
- [48] D.L. Dexter, *J. Chem. Phys.* 21 (1952) 836.
- [49] G.A. Crosby, J.N. Demas, *J. Phys. Chem.* 75 (1971) 991.
- [50] P. Thanasekaran, T. Rajendran, S. Rajagopal, C. Srinivasan, R. Ramaraj, P. Ramamurthy, B. Venkatachalapathy, *J. Phys. Chem. A* 101 (1997) 8195.
- [51] T. Rajendran, S. Rajagopal, C. Srinivasan, P. Ramamurthy, *J. Chem. Soc. Faraday Trans.* 93 (1997) 3155.